The Alba Field ocean bottom cable seismic survey: Impact on development

M. K. MacLeod, R. A. Hanson, and C. R. Bell, Chevron UK Ltd., Aberdeen, Scotland
S. McHugo, Schlumberger Oil Field Services, Gatwick, England

Alba Field, in the Central North Sea (UK Block 16/26), consists of Eocene-age, high-porosity, unconsolidated turbidite channel sands sealed by low-permeability shales at an average subsea depth of 1900 m. The main channel is approximately 9 km long and 1.5 km wide and can be up to 100-m thick (Figure 1). The channel contains discrete bodies of intrareservoir shales that can cause significant drilling, completion, and production problems. Immediately overlying the main Alba sand channel, several wells have encountered thin, discontinuous, oil-saturated Brioc sands.

Oil production is from 15 horizontal wells drilled from a single platform at the northern end of the field. Since December 1993, the field has produced 130 million barrels of oil. The field is currently producing approximately 80 000 b/d. Pressure is maintained by water injection from four injector wells. Development drilling is ongoing, and several new wells are planned.

For efficient reservoir drainage, it is vital that the horizontal wells be as close to the top of the reservoir as possible. Therefore we need accurate maps of the top of the oil-filled sandstone and the location of the intrareservoir shales. These maps and shale volumes are also needed for an accurate oil-in-place estimate. Unfortunately, a low *P*-wave impedance contrast between reservoir sand and shale makes this mapping extremely difficult on conventional *P*-wave seismic data.

The challenge is to improve the seismic image at Alba to allow accurate placement of horizontal wells and better estimates of oil in place. Furthermore, as we drill more wells close to existing producing and injector wells, we want to be able to predict water saturation ahead of the bit using 4-D seismic analysis. The Alba partnership decided to try the new four-component ocean-bottom-cable (OBC) technology to (1) obtain a clearer image of the reservoir using converted shear waves and (2) predict water saturation changes by comparing old and new *P*-wave seismic data.

The idea to use converted shear waves to image low *P*-impedance reservoirs is not new. Recently, Margrave reported success finding channel sands using V_P/V_S ratios derived from a three-component survey in Blackfoot Field. However, we feel the results presented here show that the Alba survey is the first 3-D OBC survey in which successful converted-wave imaging of the reservoir has created a significant economic benefit.

In this paper, we first overview the data, techniques, and studies used to justify the 3-D OBC survey. Next, we present images of the new OBC and reprocessed streamer seismic data that show 4-D, AVO, and converted-wave results. Finally, we suggest a new, preliminary interpretation of the Alba reservoir that is supported by two recently drilled wells.

Editor's note: The material in this paper was presented at the 1999 Offshore Europe Conference in Aberdeen, Scotland, in September 1999. A fuller version of this article was printed in the 1999 OTC Proceedings. *The following is reprinted with permission and has been edited to conform to* TLE *style.*

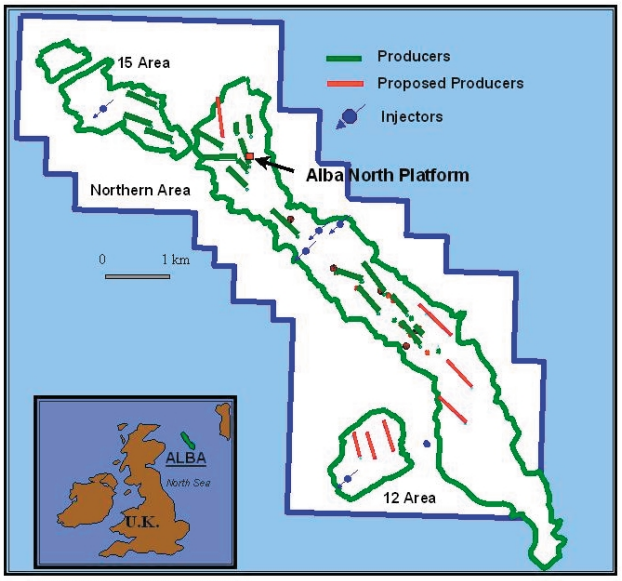

Figure 1. Alba Field in the North Sea.

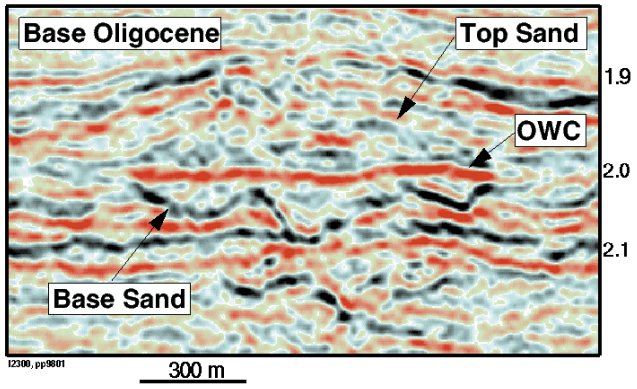

Figure 2. Conventional streamer *P*-wave image of the Alba channel. Note the strong oil-water-contact reflector and the weak top sand event. The top sand is usually interpreted to be subparallel to the base Oligocene seismic event, with the channel having an overall lens-shaped cross-section.

Methods. Several presurvey technical studies convinced the partnership (and ourselves) that a full-field 4-C OBC survey was warranted. These involved rock physics studies of the properties of the oil- and water-filled sands, seismic modeling, VSP data analysis, and ultimately 2-D OBC field trials.

4-D models. Over many parts of Alba Field, a strong seismic event on 1989 streamer seismic data corresponds to the depth of the oil-water contact (Figure 2). There was some debate as to whether this event was related to differences in diagenesis or was caused by an impedance change related to fluid differences. Therefore, to assess whether 4-D changes could be seen, we first needed to understand the cause of this reflector.

Sonic logs from the field show a velocity increase of

Table 1. Alba petroacoustic properties

	Velocity			Density			Impedance		
	mean	std	n	mean	std	n	mean	std	n
Postreservoir shales	7798	599	11360	2.20	.08	18944	17184	1444	9662
Intrareservoir shales	7659	878	864	2.19	.06	4694	16737	2085	864
Alba reservoir sand									
— Oil	8424	519	4583	2.00	.05	12146	17156	1084	3853
— Transition	9029	585	319	2.06	.05	197	18926	1398	197
— Water	9337	532	1507	2.07	.04	1901	19506	1346	1366
Prereservoir shales	8056	837	8421	2.27	.07	10212	18320	2225	8420

10% 3%

roughly 9% at the oil-water contact with very little corresponding porosity change (Figure 3). Likewise, core measurements on Alba sand showed an average increase in *P*-wave velocity of 6-7% with a change in water saturation from 7% to about 60% (Figure 4). This confirms that the velocity contrast at the oil-water contact is due to a compressibility contrast between Alba oil and brine.

We built 3-D seismic models by populating the model space with velocities and densities using geostatistical interpolation methods. This ensures a representative, heterogeneous distribution of impedance values in each region of the model (oil leg, water leg, and surrounding shales). The postproduction model incorporated the water-saturation distribution output from the Eclipse reservoir simulator. The reservoir and seismic modeling processes were significantly easier because Chevron's modeling environment is based on a shared-earth model developed in GOCAD.

The synthetic seismic models predict that the oil-water contact will dim beneath producing wells but that a residual reflection at the original oil-water contact would remain (Figure 5). In some cases a new oil-water-contact reflector is generated but, because the contrast in water saturation is not as sharp, the new reflector is not as strong as the original oil-water-contact reflector. Time pull-up due to increased water saturation is typically less than 2 ms.

AVO models. Using conventional *P*-wave seismic data to image shale-oil sand interfaces in the Alba reservoir is extremely difficult because the oil sands and shales have, on average, the same acoustic impedance (Table 1). However, a dipole sonic log from Alba shows a significant contrast in shear-wave velocities at the top and bottom of the reservoir (Figure 6). This velocity and density distribution gives rise to a class 2 AVO anomaly at top sand whereby the near-offset reflectivity is slightly positive, the far-offset reflectivity is negative, and the stacked response shows a very weak event (Figure 7). This suggests that either near-offset or far-offset seismic volumes would provide better images of the Alba sand than the conventional *P*-wave stack.

Converted wave models. Consistent with the dipole sonic log above, synthetic seismic models show a strong converted-wave (*P*-to-*S*) seismic event at the top and base reservoir (Figure 8). The model also shows no oil-water-contact reflection and a brightening of amplitudes due to tuning when the reservoir is relatively thin. Conversely, the conventional *P*-wave response shows a bright oil-water-contact event and a weak or nonexistent top and base sand event.

VSP data. Several VSP surveys show upgoing and downgoing converted-wave arrivals on the horizontal component (Figure 9). Some of the strongest converted-wave energy is being generated at the top reservoir. This gave further encouragement that an ocean-bottom cable might record these strong converted waves.

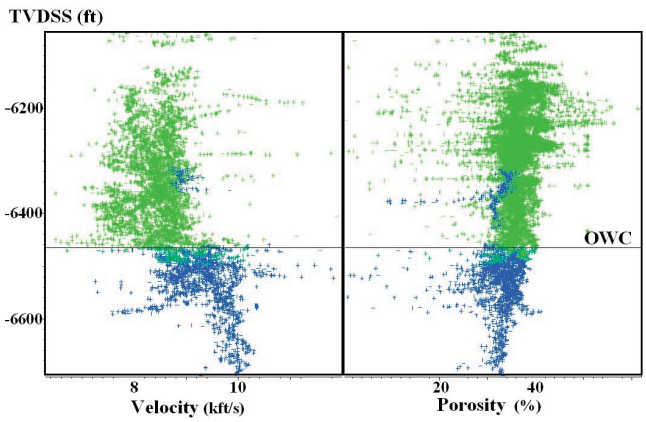

Figure 3. Wireline log response of the Alba reservoir sands, showing a strong increase in velocity at the oil-water contact with little corresponding change in porosity. This suggests the velocity increase is due to fluid compressibility differences between Alba oil and brine.

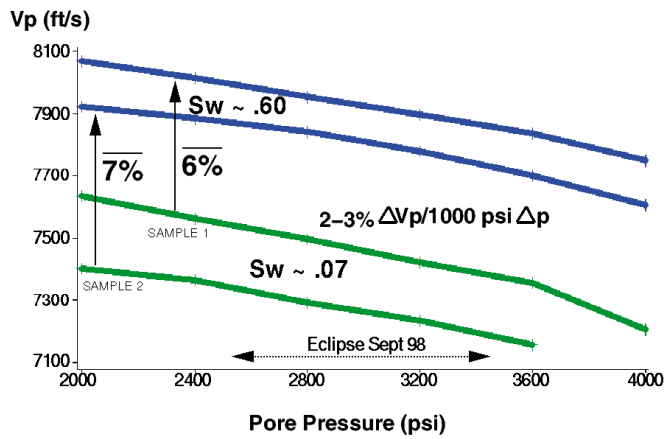

Figure 4. Measurements of *P*-wave velocity as a function of pore pressure for two core samples from Alba Field. This shows that the velocity increase seen at the oil-water contact (Figure 3) is a result of compressibility differences between Alba oil and brine.

2-D OBC field trials. Due to the results from seismic modeling and VSP data, we acquired a 2-D OBC test line with two different contractors. Although we found significant differences in vector recording fidelity between different recording systems, both produced sections with very high quality converted-wave energy. The *P*-wave OBC data were found most comparable to the 1989 streamer data when using Geco-Prakla's Nessie4C* Multiwave Array seabed system (Figure 10). These field

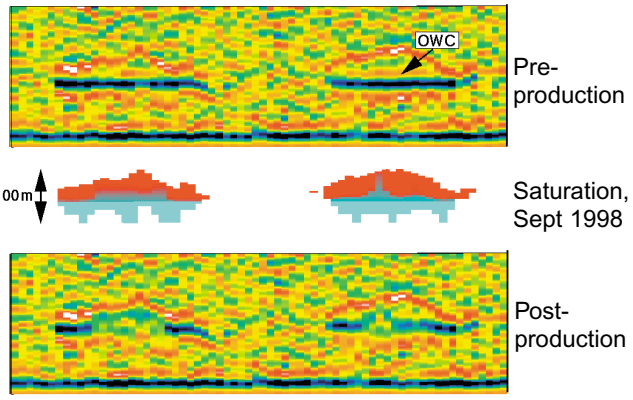

Figure 5. Pre- and postproduction synthetic seismic models showing large changes in the oil-water contact.

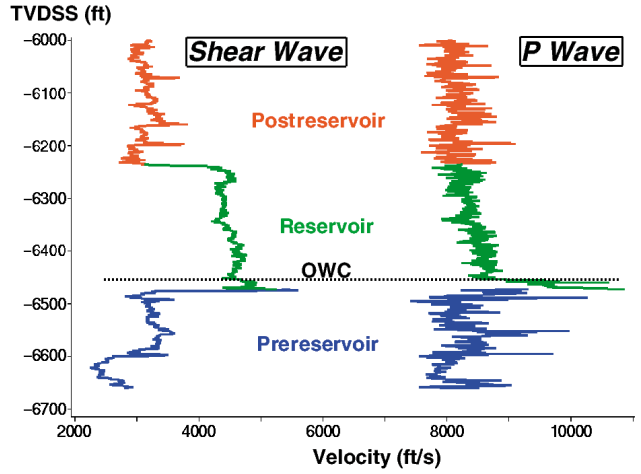

Figure 6. Dipole sonic log through the Alba reservoir sand showing a large contrast in shear-wave velocity and a small contrast in *P*-wave velocity with the surrounding shales.

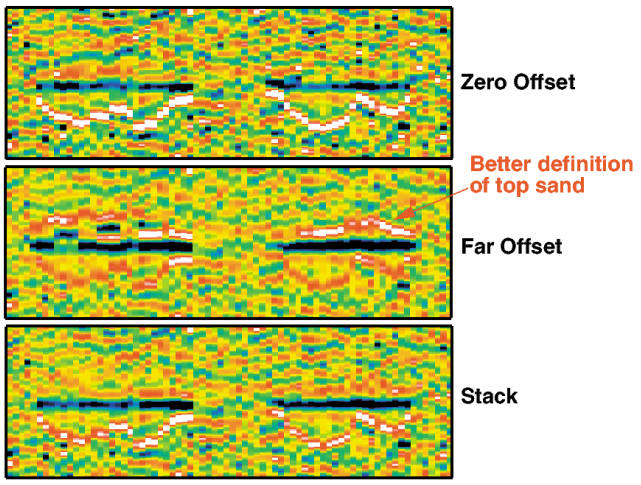

Figure 7. AVO seismic models of the Alba channel. The far-offset *P*-wave image shows the top sand reflection better than the stacked response.

trials demonstrated that: (1) high-quality converted-wave data could be acquired and processed quickly and (2) the *P*-wave and converted-wave sections could be charactertied, allowing depth predictions on the converted-wave data.

3-D full-field OBC survey. Based on the technical studies described above and a cost-benefit study, Chevron commissioned Geco-Prakla to acquire a 67 km^2 3-D multicomponent survey in early 1998. The survey was recorded in 14 swaths parallel to the 1989 streamer survey (Figure 11). The choice of swath acquisition geometry over orthogonal geometry was based on our desire to produce a data set that was relatively easy to process and was similar to the streamer survey to avoid problems with 4-D analysis. Acquisition took eight weeks in rough weather. Processing of the initial converted-wave cube took only three-and-a-half months. The total acquisition and processing cost was less than the cost of one trouble-free horizontal well.

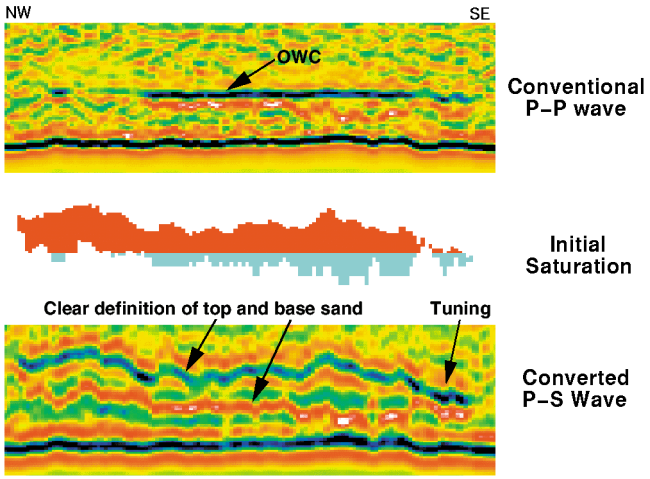

Figure 8. *P*-wave and converted-wave synthetic seismic model of the Alba reservoir. The *P*-wave results show a strong event at the OWC. The converted-wave model shows strong events at the top and base of the producing sand but no reflection at the OWC.

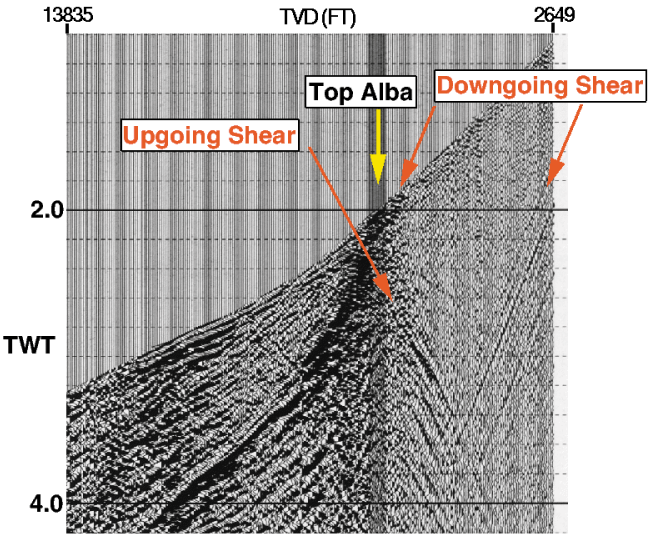

Figure 9. VSP from Alba showing strong up- and downgoing shear-wave energy.

Results. The key results of the OBC survey included:

4-D changes. *P*-wave seismic sections near two injector wells show large differences between the pre- and postproduction surveys (Figure 12). Here, the oil-water contact appears to have disappeared completely. We also see an apparent brightening in the top reservoir reflector where the contrast between the overlying shales and the reservoir sand has been enhanced by the higher water satura-

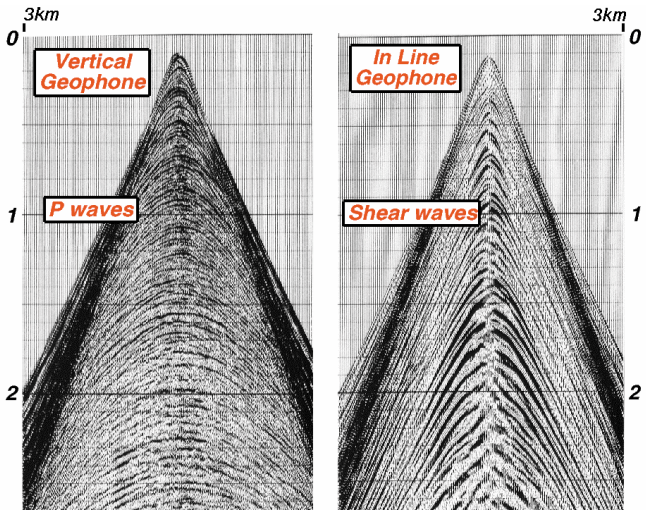

Figure 10. Common receiver gathers from the 2-D OBC test. Note the excellent separation between the *P*-wave energy on the vertical phone and the converted shear-wave energy on the in-line phone.

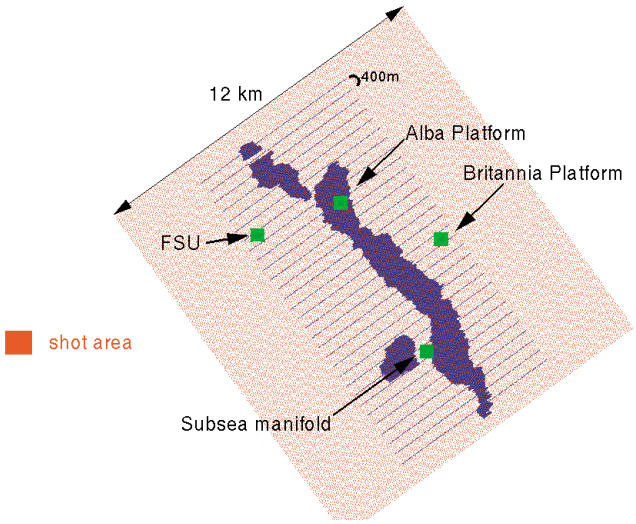

Figure 11. Presurvey acquisition plan for the 3-D OBC survey. The 6-km receiver lines were laid out in pairs, 400 m apart. The obstacles would have made streamer acquisition very difficult.

tion. In other parts of the field, the oil-water contact is now significantly higher than the original depth (Figure 13). In a few isolated areas, the oil-water contact is actually deeper than the original depth by approximately 10 m, consistent with Eclipse saturation distributions.

AVO results. In some parts of the field, the far-offset *P*-wave image of the reservoir is superior to the full-offset image (Figure 14). The top reservoir event is more obvious, and we see unusual reflections at the channel edge. These winglike features appear in some cases to be sands injected along fault planes that define the channel margin.

Converted-wave results. In almost every part of the field, converted-wave data show an improved image of the reservoir sands compared with the *P*-wave seismic image (Figure 15). The reservoir is characterized by high-amplitude reflections at almost double the *P*-wave traveltimes. At depths corresponding to the Britannia Gas Field (3700 m), the converted-wave data have relatively poor resolution (Figure 16). At the Alba reservoir level, the wavelength of the converted-wave data is about 30% longer than

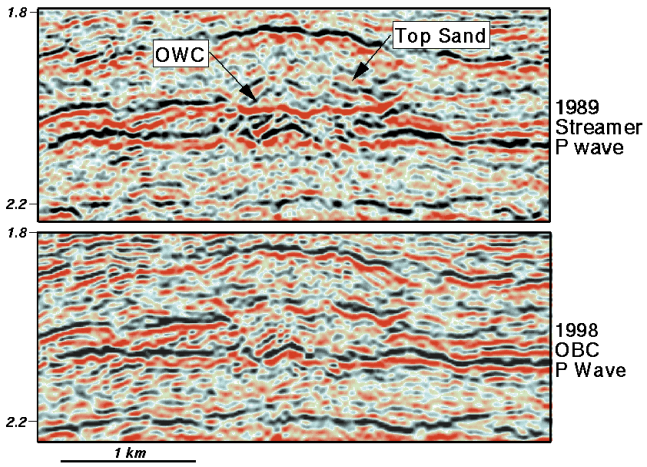

Figure 12. Pre- and postproduction seismic data showing significant differences in the oil-water-contact event. Note the excellent repeatability of the streamer and OBC seismic data and the brighter top sand event in the OBC data.

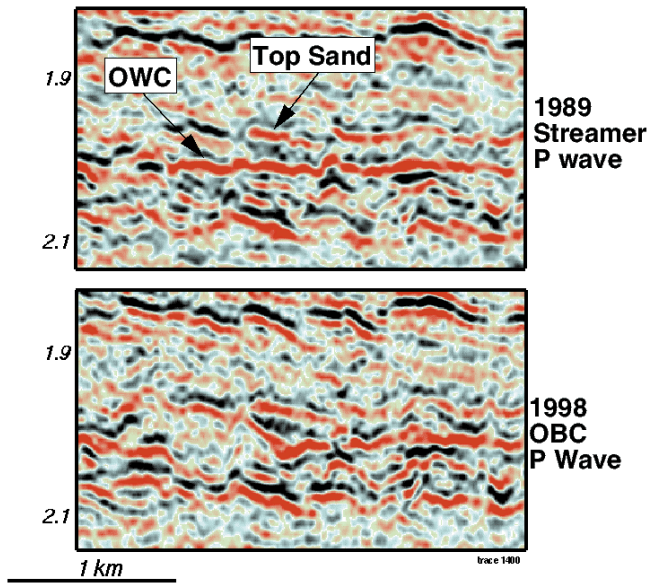

Figure 13. Pre- and postproduction seismic data showing a raised oil-water contact near a fault. To the right of the fault it appears that the oil-water contact is lower than the original contact.

the wavelength of the *P*-wave data. However, converted-wave images of the reservoir sands show features not observable in traditional single-component data. These include:

- high-amplitude top and base sand reflectors (Figure 17)
- discontinuous sand reflectors. (Such discontinuities may correspond to faults visible within the postreservoir *P*-wave seismic data but could also indicate "subchannels" within the main Alba channel system.)
- "wing" features in the top sand reflector at the channel edges and occasionally over the central axis of the channel (Figure 18). As opposed to the downward-dipping concave lens structure previously interpreted using the *P*-wave data, the converted-wave data frequently show upward-dipping high-amplitude events at the channel margins.

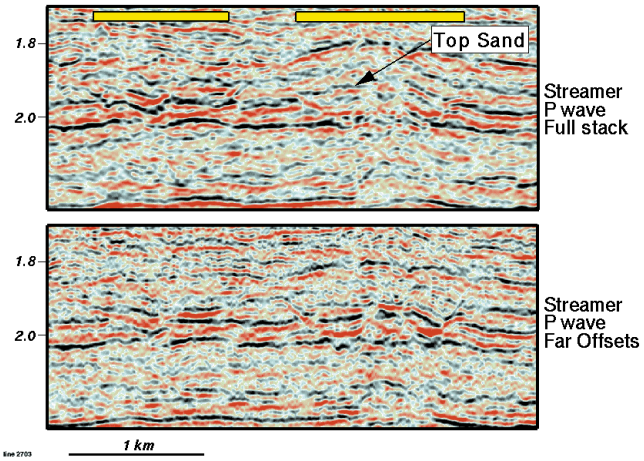

Figure 14. Far-offset streamer data show a clearer image of the top and margins of the Alba channel.

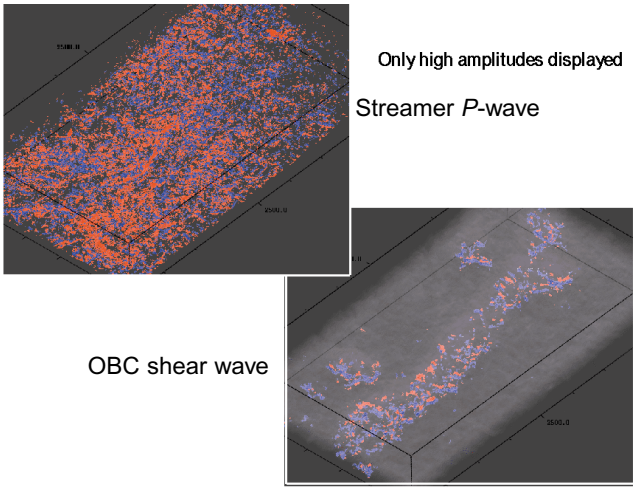

Figure 15. 3-D view of the streamer and converted-wave OBC data over Alba Field. In each display, a subvolume of the original data is displayed with only the high amplitudes visible. The outline of the field is clearly seen only in the converted-wave data.

The strong converted-wave reflectors encouraged us to invert the new seismic data to a "pseudoelastic impedance." While the computed impedance is not a direct earth property, it appears to tie well lithologies and promises a method for predicting sands and shales in the reservoir interval (Figure 19). The impedance data also make structural interpretation easier by improving correlations along the top and base sand.

Recent well results. Two successful wells have been drilled this year based primarily on the interpretation of the new converted-wave data. Both were placed at the margins of the main channel and have validated the presence of the wings. The first well (A29) was drilled in the northern part of the field in an area characterized by large intrareservoir shale bodies (Figure 20). The well first encountered 150 m of oil-saturated sands within a young postreservoir shale section before drilling roughly 550 m of sand in the main reservoir. We interpret the first sand as being injected into the overlying shales some time after deposition. The well has been producing at rates of up to 20 000 b/d for the last two months.

The second well (A30), drilled on the western flank of the field, encountered 700 m of sand and only 30 m of intrareservoir shale (Figure 21). This has resulted in Alba's highest-net sand well (over 96%). An initial pilot well showed that the wing in this part of the field is 20 m thick. This well is currently being completed.

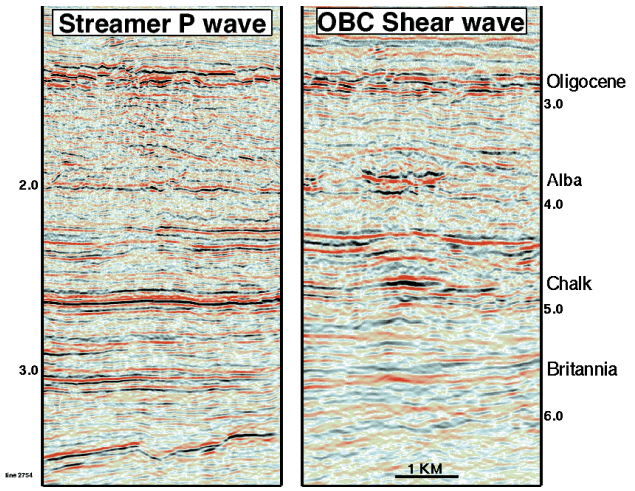

Figure 16. Streamer data compared with converted-wave data from near the central part of the field. At the reservoir level, the converted-wave image is far superior to the *P*-wave image. At the Britannia level, the *P*-wave image is superior.

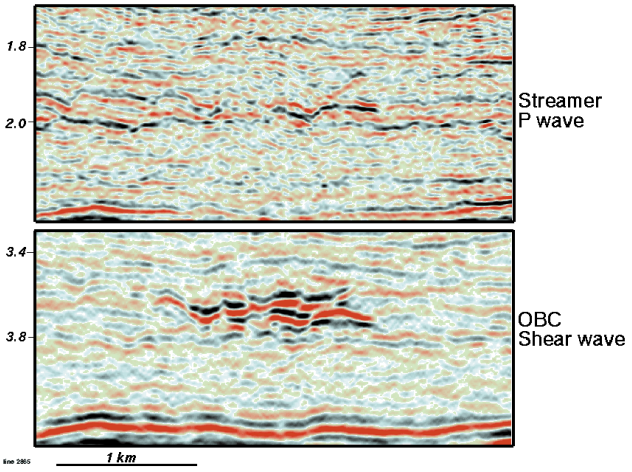

Figure 17. Converted-wave image from the "15 Area" (see Figure 1) showing dramatically improved imaging relative to the streamer *P*-wave data.

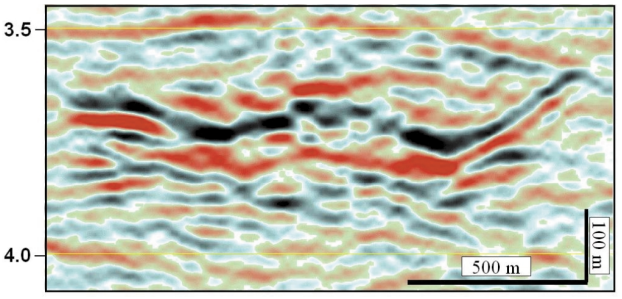

Figure 18. Converted-wave image from the central part of the field showing "wings" which may represent postdepositional deformation and injection of the sand into the overlying and adjacent shales.

Geologic model. These new wells and the complex geometry of the Alba channel seen on the new converted-wave seismic data suggest significant postdepositional deformation of the turbidite channel. Core data from Alba also

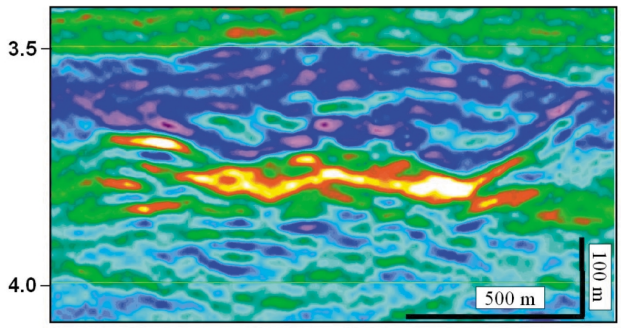

Figure 19. Pseudoelastic impedance inversion of section in Figure 18.

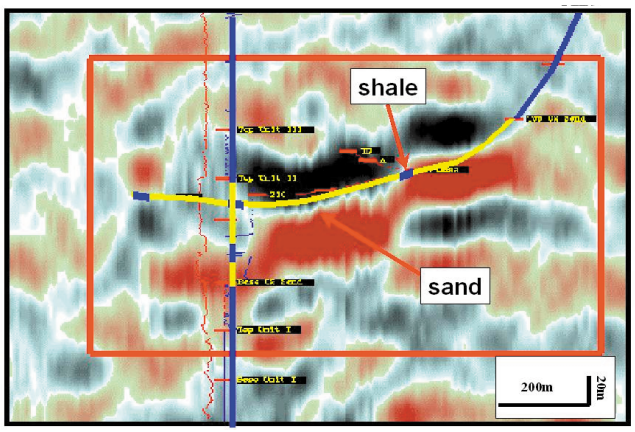

Figure 20. Converted-wave seismic line through well A29 showing excellent tie between lithologies encountered in the well and the seismic response.

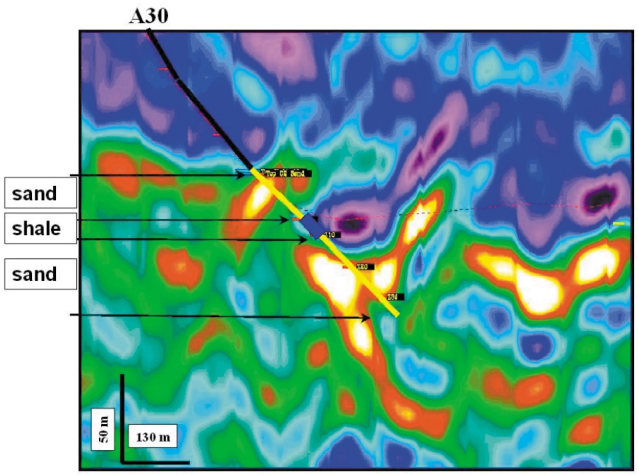

Figure 21. Pseudoelastic impedance through well A30 showing excellent tie between lithologies encountered in the well and impedance.

show remobilization and injection of Alba sands into the overlying shales. The central axis of the channel is often flanked by synclines that may represent sand-withdrawal features (e.g., Figure 18). We now believe that many thin Brioc sands overlying the main channel have been injected out of the main channel. More detailed mapping and future wells will help us evaluate this hypothesis.

Data management and integrated interpretation. Numerous 3-D seismic volumes (more than 40 to date) have been generated from the 3-D streamer and OBC seismic surveys at Alba. The richness of the 3-D, 4-C data allows various auxiliary cubes to be derived from the primary data sets. These

additional cubes are important because rock and fluid properties can be obtained from the different seismic volumes. For example, the OBC *P*-wave data are better for mapping changes in the oil-water contact, whereas converted-wave data are better for mapping the sand-body geometry. Inversion of the converted-wave data allows improved interpretability and lithology prediction. Faults above the reservoir are better resolved on the reprocessed streamer data, but coherency cubes derived from both *P*-wave and converted-wave data are valuable for imaging various kinds of discontinuities: faults, sand channel boundaries, and fluid contacts. The difference cube (streamer minus *P*-wave OBC data) quickly shows the more obvious water-saturation changes.

The key technical and work flow challenge is to provide a simultaneous integrated interpretation of all data volumes. Some benefits of such an interpretation are more confident correlation of the top and base reservoir sands leading to accurate well placement, better oil-in-place estimates, better fault correlations, sand and shale lithology mapping, fluid contact mapping, and 3-D estimates of Poisson's ratio. New developments in interpretation software are needed to enable efficient handling of these multiple data volumes and the time differences between *P*-wave and converted-wave data. Combining these seismic volumes accurately and efficiently with well data is crucial to meeting the challenge.

Conclusions. The presurvey technical studies and field trials were critical to our understanding of the rock properties and expected reflection characteristics of the new OBC seismic data. The studies also helped convince us of the technical merits of applying this new technology at Alba Field.

The interpretation of the converted-wave cube is now a critical component of our understanding of the structure of the Alba reservoir. This interpretation is the primary input for the construction of a new full-field reservoir model. Finally, the converted-wave data are now central to the well planning and geosteering processes.

Time-lapse changes seen in the new *P*-wave data are changing our understanding of fluid flow and are impacting well placement. Far-offset *P*-wave data support the interpretation of significant postdepositional deformation of the Alba turbidite channel.

The full benefit of these new data will be realized by the integrated interpretation of many seismic volumes generated from the old and new surveys along with log and core data. New tools and interpretation methodologies are needed to achieve this complete integration. Future work at Chevron will focus on making accurate depth predictions from the converted-wave data and improving converted-wave imaging with prestack depth migration.

With the first well being drilled less than a year after seismic acquisition started, the new data arrived in time to make a significant commercial impact on the field's development. We hope our results at Alba will cause further development and more widespread use of this exciting new technology.

Suggestions for further reading. "The Alba Field: Evolution of the depositional model" by Newton and Flanagan (*Petroleum Geology of Northwest Europe: Proceedings of the 4th Conference*, 1993). "Interpreting channel sands with 3C-3D seismic data" by Margrave et al. (*TLE*, 1998). "Multicomponent analysis of OBC data" by MacLeod et al. (1999 *OTC Proceedings*). "Acquisition and processing of 3-D multicomponent seabed data from Alba Field—a case study from the North Sea" by McHugo et al. (1999 EAGE Annual Technical Conference). "Polygonal faults and their influence on deepwater sandstone reservoir geometries, Alba Field" by Lonergan and Cartwright (AAPG *Bulletin*, 1999). "Multicomponent seismic interpretation: Data integration issues, Alba Field, North Sea" by Hanson et al. (1999 EAGE Annual Technical Conference). "Simultaneous visualization of 3-D multicomponent seismic data, Alba Field, North Sea" by Thompson et al. (1999 EAGE Annual Technical Conference).

Acknowledgments: The authors thank the Alba partnership (Chevron, Arco, Conoco, Fina, Petrobras, Saga, Statoil, and Unilon/Baytrust) for its support in acquiring the survey and for permission to publish this paper. At Chevron, Kelvin Reynolds and Mike Hadley directed most aspects of the acquisition and data processing with their counterparts at Geco-Prakla, Mike Hodge and Tony Probert. Kameron Mitchell provided guidance regarding the reservoir management implications and cost/benefits of a new 3-D survey. Mark Sawyer, Sheila Groves, and Chris Thompson of Chevron and Jorgen Somod of Saga U.K. supported this work through technical analysis and discussion. We also thank our colleagues at Chevron Petroleum Technology Company, specifically Zhijing Wang (rock physics), Ron Behrens (reservoir modeling), Ali Tura (AVO and shear modeling), David Lumley (4-D and shear modeling) [both Tura and Lumley now at 4th Wave Imaging], Clint Frasier (converted-wave processing and interpretation), and Greg Surveyor, Harry Martin, and Rich Alford (4-D equalization). Jason Geosystems performed the converted-wave inversion work.

Corresponding author: M. K. MacLeod, kmac@chevron.com